# Self-trapped atomic matter wave in a ring cavity

Jieli Qin [*]

*School of Physics and Materials Science, Guangzhou University, 230 Wai Huan Xi Road, Guangzhou Higher Education Mega Center, Guangzhou 510006, China*

Lu Zhou [†]

*Department of Physics, School of Physics and Electronic Science, East China Normal University, Shanghai 200241, China and Collaborative Innovation Center of Extreme Optics, Shanxi University, Taiyuan, Shanxi 030006, China*

We studied a system of atomic Bose-Einstein condensate coupled to a ring cavity within the mean-field theory. Due to the interaction between atoms and light field, the atoms can be self-trapped. This is verified with both variational and numerical methods. We examined the stability of these self-trapped states. For a weakly pumped cavity, they spread during the evolution; while at strong pumping, they can maintain the shape for a long time. We also studied the moving dynamics of these self-trapped waves, and found out that it can be strongly affected by the cavity decay rate. For a small cavity decay rate, the self-trapped waves undergo a damped oscillation. Increasing the cavity decay rate will lead to a deceleration of the self-trapped waves. We also compared the main results with the semiclassical theory in which atoms are treated as classical particles.

## I. INTRODUCTION

Self-trapping is a ubiquitous phenomenon in nature; for example, solitons in various systems [1–6], and liquid helium droplets [7] are all some kind of self-trapped state. The highly tunable atomic Bose-Einstein condensate (BEC) provides an ideal platform for studying such phenomena. In the BEC system, the attractive interatom interaction (*s*-wave collision) results in a Kerr type self-trapping nonlinearity [8], and can support bright solitons [9–11]. If quantum fluctuation (Lee-Huang-Yang correction [12]) is included, self-trapped droplets can also be formed in the BEC system [13–17].

Interacting with electromagnetic fields can also lead to nonlinearity in the BEC systems. When a BEC is illuminated by electromagnetic waves, it feels a potential from the electromagnetic field. At the same time, the BEC also serves as a medium, and will backwardly affect the propagation of the electromagnetic waves. The affected electromagnetic field will in turn further affect the dynamics of BEC. Due to this feedback mechanism, nonlinear features arise in the system. Many interesting phenomena resulting from this type of nonlinearity have been reported [18]. For atomic gas in a cavity, because of this feedback effect, a dynamical rather than a static optical lattice is produced. In such a dynamical lattice the atoms feel a friction force, and thus can be cavity cooled and self-organized [19–21]. It also softens an optical lattice, and leads to asymmetric matter wave diffraction [22,23] and polaritonic solitons [24]. It also gives rise to phenomena such as spin-exchange [25,26] and long-range interactions [27,28],

self-structuring [29,30], photon bubbles [31,32], bistability [33–36], spin texture [37,38], chaotic dynamics [39], and parametric resonance [40] in the light-BEC interacting systems. And in the microwave-BEC interacting systems, soliton [41,42] and vortex [43] phenomena have also been reported. Most recently, it is found that due to such nonlinearity, supersolids can exist in a driven-dissipative ring-cavity-BEC system [44,45]; futhermore, a precise gravimeter has been proposed based on the system [46]. And a type of crystalline droplet has also been predicted in an atom-cavity setup. [47].

Motivated by this progress, in this work we propose that a self-trapped matter wave can also be supported by the cavity-mediated nonlinearity in a driven-dissipative cavity-BEC system, and study its stability and dynamics using the mean-field theory. In the considered system (see Fig. 1), the cavity light field is built up by transversely illuminating the BEC, then the built-up light field forms an optical lattice potential for the BEC. We theoretically demonstrated that this induced optical lattice can support a self-trapped wave packet. For a weak cavity pumping, the induced optical lattice is shallow; the localized wave packet cannot be well trapped, therefore it spreads during the time evolution. And for a strong pumping, the induced optical lattice can be strong enough to support a long-time stable self-trapped wave packet. The moving dynamics of these self-trapped waves show very different features under different cavity decay rates. This is due to the adiabaticity of the induced optical lattice. The induced optical lattice tends to follow the movement of the self-trapped wave packet; however, it cannot completely catch up. Thus, the self-trapped wave packet feels a dragging force from the induced optical lattice falling behind it, therefore it decelerates, and finally stops. When the self-trapped wave packet stops, the optical lattice also catches up, and the system

---

[*]104531@gzhu.edu.cn; qinjieli@126.com
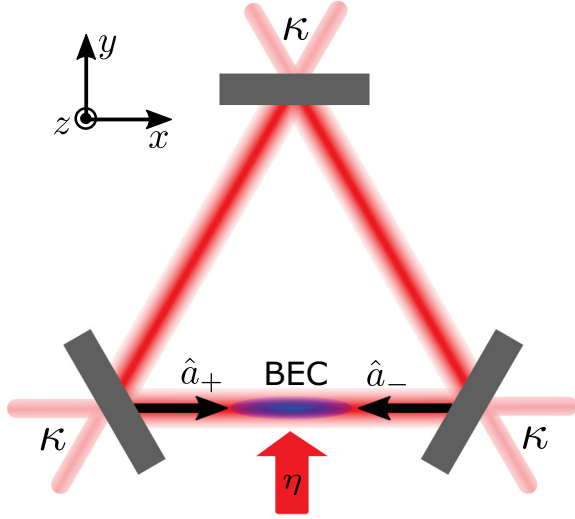[†]lzhou@phy.ecnu.edu.cn

FIG. 1. Diagram of the considered system. A quasi-one-dimensional atomic BEC is loaded into a ring cavity with loss rate $\kappa$. The BEC atoms interact with two degenerate counterpropagating modes ($\hat{a}_+$ and $\hat{a}_-$) of the ring cavity. The system is pumped by transversely shining a laser on the BEC; the pumping strength is $\eta$.

reaches a steady state. If the cavity decay rate is small, and even if the self-trapped wave packet has been decelerated to the speed of zero, the optical lattice still cannot catch up, so the self-trapped wave packet will then be accelerated in the opposite direction. The deceleration and acceleration alternately repeat several times, and overall the self-trapped wave packet displays a damped oscillation. In the bad cavity limit [48,49] (which means that the cavity decay rate is much larger than the atom-cavity coupling, the cavity light field quickly decays to a steady state, and can instantaneously follow the dynamics of BEC), the self-trapped wave packet feels no dragging force and will constantly move with the initial given speed. At last, we point out that in different atom-cavity setups the phenomena of self-organization and friction force on atoms are also predicted by the semiclassical theory in which the atoms are treated as classical particles [20,21]. But here by using the mean-field theory, the atoms are described by a Schrödinger-like equation, thus the effects of quantum pressure and tunneling of atoms to neighboring lattice sites can also be included.

The paper is organized as follows: In Sec. II, the physical model studied in this paper is presented. In Sec. III, we show the existence of self-trapped wave packets in the system with both the variational method and numerical simulation. Examples of the self-trapped wave packets and their stability are also shown in this section. In Sec. IV, the moving dynamics of the self-trapped wave packets are studied in detail. And, we briefly compare the main results obtained using mean-field theory with their semiclassical correspondences in Sec. V. Finally, the paper is summarized in Sec. VI.

## II. MODEL

We consider a ring cavity-BEC coupling system [44] which is schematically shown in Fig. 1. A two-level atomic BEC is trapped along the cavity axis by a tight transverse confin-

ing potential, and thus can be reduced to one-dimensional. The atoms are driven in the transverse direction by an off-resonant (with detuning $\Delta_a$) pump laser, which induces a Rabi oscillation of frequency $\Omega_0$ between the two internal atomic states. The transition between the two atomic energy levels is also off-resonantly coupled to the two counterpropagating cavity modes $\hat{a}_\pm e^{ik_c x}$ ($k_c$ is the wave number of the cavity modes) with strength $\mathcal{G}_0$. In the far-off-resonant regime $|\Delta_a| \gg \Omega_0, \mathcal{G}_0$, the excited atomic state can be adiabatically eliminated, and in the rotating frame of the pump laser, the system can be described by the following effective Hamiltonian:

$$\mathcal{H} = -\hbar\Delta_c(\hat{a}_+^\dagger\hat{a}_+ + \hat{a}_-^\dagger\hat{a}_-) + \int \hat{\psi}^\dagger H_a \hat{\psi}\, dx, \quad (1)$$

where the first term describes the two counterpropagating cavity modes, and the second term accounts for the BEC and its interaction with the light field. In this equation, $\hbar$ is the Planck constant, $\Delta_c$ is the detuning between the cavity modes and pump laser, $\hat{\psi}$ is the field operator of the BEC, and $H_a$ is the corresponding single-particle Hamiltonian

$$H_a = \frac{\hat{p}^2}{2m} + V_{ac} + V_{ap}, \quad (2)$$

with

$$V_{ac} = \hbar U_0[\hat{a}_+^\dagger\hat{a}_+ + \hat{a}_-^\dagger\hat{a}_- + (\hat{a}_+^\dagger\hat{a}_- e^{-2ik_c x} + \text{H.c.})], \quad (3)$$

$$V_{ap} = \hbar\eta_0(\hat{a}_+ e^{ik_c x} + \hat{a}_- e^{-ik_c x} + \text{H.c.}). \quad (4)$$

Here, $\hat{p}^2/2m$ is the kinetic energy of the BEC atom, $V_{ac}$ is the optical potentials due to two-photon scattering between the two cavity modes, and $V_{ap}$ is the optical potential due to two-photon scattering between the pump and cavity modes. The meanings of the symbols are as follows: $m$ is the mass of the BEC atom, $\hat{p} = -i\hbar\frac{\partial}{\partial x}$ is the momentum operator, $U_0 = \hbar\mathcal{G}_0^2/\Delta_a$ describes the strength of optical potential $V_{ac}$, and $\eta_0 = \hbar\mathcal{G}_0\Omega_0/\Delta_a$ is the effective cavity pump strength. In the following contents, natural unit $m = \hbar = k_c = 1$ will be applied for simplicity, i.e., the length, time, velocity, and energy will be measured in units of $1/k_c$, $m/(\hbar k_c^2)$, $\hbar k_c/m$, and $\hbar^2 k_c^2/m$.

The BEC usually contains a large number of atoms. To support the self-trapped wave, which is the main subject of this paper, a strong light field is also needed. Thus, the mean-field approximation [50] can be adopted (in Ref. [45] which considers a very similar system, the mean-field results fit the experimental preservation well). The quantum mechanical operators can be approximated by their corresponding mean value $c$ numbers, $\hat{a}_\pm \to \alpha_\pm$ and $\hat{\psi} \to \psi$. We further scale $\alpha_\pm$ and $\psi$ with the total atom number $N$, i.e., $\alpha_\pm \to \alpha_\pm/\sqrt{N}$, $\psi \to \psi/\sqrt{N}$. Using such a scaling, the norm of the wave function $\psi$ becomes

$$\int |\psi(x)|^2 dx = 1.$$

And we also introduce new parameters $\eta = \sqrt{N}\eta_0$ and $U = U_0 N$ to account for the many atoms. The equations governing the dynamics of these mean-field variables can be obtained

by taking the mean values of the corresponding Heisenberg equations

$$i\frac{\partial}{\partial t}\alpha_\pm = (-\Delta_c + U - i\kappa)\alpha_\pm + UN_{\pm 2}\alpha_\mp + \eta N_{\pm 1}, \quad (5)$$

$$i\frac{\partial}{\partial t}\psi = \left[-\frac{1}{2}\frac{\partial^2}{\partial x^2} + \mathcal{V}_{\text{eff}}(x)\right]\psi, \quad (6)$$

where the cavity loss with rate $\kappa$ has been introduced phenomenologically, and for conciseness of the equations, here we also defined the following quantities:

$$N_{\pm 1} = \int |\psi(x)|^2 e^{\mp ix} dx,$$

$$N_{\pm 2} = \int |\psi(x)|^2 e^{\mp 2ix} dx,$$

$$\mathcal{V}_{\text{eff}}(x) = \mathcal{V}_{ac}(x) + \mathcal{V}_{ap}(x),$$

$$\mathcal{V}_{ac} = U(|\alpha_+|^2 + |\alpha_-|^2) + U(\alpha_+^* \alpha_- e^{-2ix} + \text{c.c.}),$$

$$\mathcal{V}_{ap} = \eta(\alpha_+ e^{ix} + \alpha_- e^{-ix} + \text{c.c.}).$$

Letting $\frac{\partial}{\partial t}\alpha_\pm = 0$ and $\psi(x,t) = \psi(x)e^{-i\mu t}$ with $\mu$ being the BEC chemical potential, the steady state of the system follows equations

$$\mu\psi(x) = \left[-\frac{1}{2}\frac{\partial^2}{\partial x^2} + \mathcal{V}_{\text{eff}}(x)\right]\psi(x), \quad (7)$$

$$\alpha_+ = -\frac{(-\Delta_c + U - i\kappa)\eta N_{+1} - \eta U N_{+2} N_{-1}}{(-\Delta_c + U - i\kappa)^2 - U^2 N_{-2} N_{+2}}, \quad (8)$$

$$\alpha_- = -\frac{(-\Delta_c + U - i\kappa)\eta N_{-1} - \eta U N_{-2} N_{+1}}{(-\Delta_c + U - i\kappa)^2 - U^2 N_{-2} N_{+2}}. \quad (9)$$

Here we point out that Eqs. (8) and (9) also describe the cavity field amplitudes of the system in the bad cavity limit [48,49]. In the bad cavity limit, the cavity light field quickly decays to the steady state, then $\partial_t \alpha_\pm \approx 0$ can be approximately applied, so Eqs. (8) and (9) hold. Together with Eq. (6), the dynamics of the cavity-BEC system in the bad cavity limit can be described.

At last, we see that the dynamics of the BEC macroscopic wave function are governed by a Schrödinger-like equation, Eq. (6). This equation is a nonlinear one, since the optical potentials $\mathcal{V}_{ac}(x)$ and $\mathcal{V}_{ap}(x)$ felt by the BEC recursively depend on the wave function $\psi$ of the condensate. This nonlinearity can support self-trapped waves in the system, which will be discussed in the next section.

## III. SELF-TRAPPED MATTER WAVE

In the system, a super-radiation phase transition takes place at the critical pumping strength [44]

$$\eta_c = \sqrt{\frac{(-\Delta_c + U)^2 + \kappa^2}{8(-\Delta_c + U)}}. \quad (10)$$

Below the critical pumping strength ($\eta < \eta_c$), the cavity light field is almost zero ($\alpha_\pm \approx 0$); the atoms feel a negligible optical potential, and will have a uniform distribution. However, above the critical pumping strength ($\eta > \eta_c$), a considerable intensity of cavity field can be built up, hence the optical lattice potential acting on the atoms will play a crucial role.

And it will be natural to think that this induced optical lattice potential can support a self-trapped matter wave packet. This will be verified by both the variational method analysis and numerical simulation in the following contents of this section.

To simplify the variational calculation, we further neglect the terms related to $U, UN_{\pm 2}$ (i.e., terms due to two-photon scattering between the two cavity modes) in Eqs. (8) and (9) under the assumption $\kappa \gg U, UN_{\pm 2}$. And the simplified optical field reads

$$\alpha_\pm \approx \frac{\eta N_{\pm 1}}{\Delta_c + i\kappa}. \quad (11)$$

We see the optical field is determined by the two-photon scattering between the pump and cavity modes. Then, the ratio between the amplitudes of the two optical potentials $\mathcal{V}_{ac}$ and $\mathcal{V}_{ap}$ is calculated to be

$$\frac{\mathcal{V}_{ac}}{\mathcal{V}_{ap}} \sim \frac{U|\alpha_\pm|^2}{\eta|\alpha_\pm|} = \frac{U|N_{\pm 1}|}{|\Delta_c + i\kappa|} \ll 1.$$

So, compared to $\mathcal{V}_{ap}$, $\mathcal{V}_{ac}$ can be neglected. Equation (6), which governs the evolution of atomic BEC, can be simplified to the following nonlinear Schrödinger equation:

$$i\frac{\partial}{\partial t}\psi = -\frac{1}{2}\frac{\partial^2}{\partial x^2}\psi + \left[\frac{\eta^2(N_{+1}e^{ix} + N_{-1}e^{-ix})}{\Delta_c + i\kappa} + \text{c.c.}\right]\psi. \quad (12)$$

The effective Hamiltonian corresponding to this equation can be written as

$$H_{\text{eff}} = \int \hat{\psi}^\dagger(x)\left(-\frac{1}{2}\frac{\partial^2}{\partial x^2}\right)\hat{\psi}(x)dx$$
$$+ \left[\frac{\eta^2}{\Delta_c + i\kappa}\left(\int \hat{\psi}^\dagger(x_1)e^{ix_1}\hat{\psi}(x_1)dx_1\right)\right.$$
$$\left. \times \left(\int \hat{\psi}^\dagger(x_2)e^{-ix_2}\hat{\psi}(x_2)dx_2\right) + \text{H.c.}\right]. \quad (13)$$

Taking a Gaussian wave packet localized at position $x = 0$

$$\psi_{\text{va}}(x) = \left(\frac{2}{\pi\sigma^2}\right)^{1/4} e^{-(x/\sigma)^2} \quad (14)$$

as the variational trial wave function where the wave-packet width $\sigma$ is the only variational parameter, the variational energy is integrated to be

$$E_{\text{va}} = \frac{1}{2\sigma^2} + \frac{2\Delta_c\eta^2}{\Delta_c^2 + \kappa^2}\exp\left[-\frac{\sigma^2}{4}\right]. \quad (15)$$

In Fig. 2, the variational energy $E_{\text{va}}$ is plotted as a function of variational parameter $\sigma$ for different pumping strength $\eta$. We clearly see that there exists a minimal point on the $E_{\text{va}}$-$\sigma$ curve, which indicates the existence of a self-trapped wave packet. And from the figure, one also expects that the self-trapped wave packet will have a narrower width under a stronger pumping strength (a larger value of $\eta$), as the stronger pumping can produce a deeper optical lattice. These conclusions will be further verified by the numerical simulations.

Numerically, the steady state of the system is found by propagating Eqs. (6), (8), and (9) with the imaginary time method from an initial trial narrow Gaussian wave packet. Some examples of the numerically found self-trapped wave
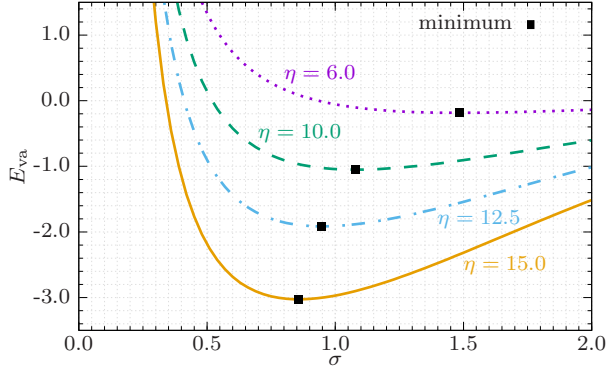
FIG. 2. Variational energy. The variational energy $E_{va}$ is plotted as a function of the variational parameter $\sigma$ (width of the wave packet) in the trial wave function (14). The four lines correspond to different pumping strengths $\eta = 6.0, 10.0, 12.5,$ and $15.0$. The black squares are the minimum points of the lines. Other parameters used are $U = -0.5$, $\Delta_c = -1$, and $\kappa = 10$.

packets and their variational counterparts for different pumping strength $\eta = 6$ (top), 10 (middle), and 15 (bottom) are shown in the left panels of Fig. 3, where the induced optical lattice potentials $\mathcal{V}_{eff}$ are also plotted. Here the optical lattices in fact have different bottom energies, but for the convenience of comparison, we shift all of them to the value of zero. We see that the variational and numerical results fit each other very well. And as the pumping strength $\eta$ increases, the depth
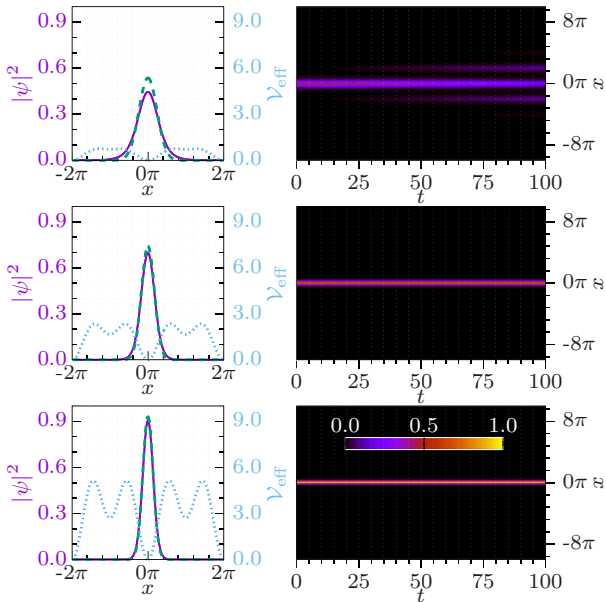


FIG. 3. Some examples of the self-trapped wave packets and their stability. Left panels: Density profiles $|\psi|^2$ of the self-trapped waves and the corresponding induced optical lattice potential $\mathcal{V}_{eff}$ for pumping strength $\eta = 6$ (top panel), 10 (middle panel), and 15 (bottom panel). The violet solid and green dashed lines are numerical and variational results for $|\psi|^2$, respectively. The cyan dotted lines are numerical results for $\mathcal{V}_{eff}$. Right panels: Corresponding time evolution of the self-trapped waves shown in the left panels. Other parameters are $U = -0.5$, $\Delta_c = -1$, and $\kappa = 10$.
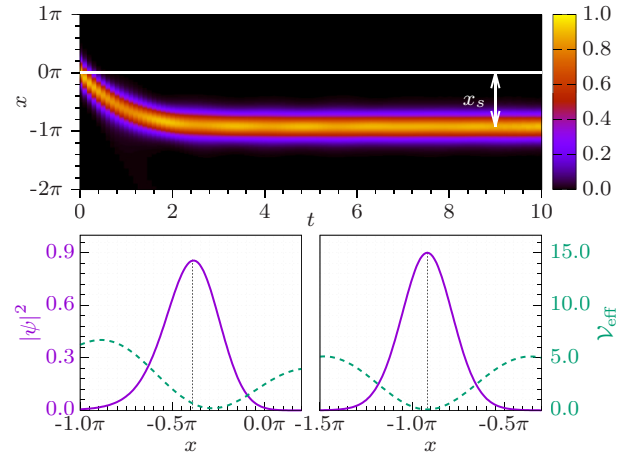


FIG. 4. Decelerating motion of the self-trapped wave packet. Initially, the self-trapped wave packet locates at $x = 0$ (white solid line), and its velocity is set to $v_0 = -3$. Top panel: The afterward evolution of the density profile. The limit traveling distance of the wave packet is $x_s = 2.88$ (white two-headed arrow). Bottom panels: The density profiles (violet solid line) and corresponding induced optical lattice potentials (green dashed line) at $t = 0.5$ (left panel) and $t = 5.0$ (right panel). The black dotted line is plotted to mark the center of the wave packet. Other parameters used are $U = -0.5$, $\Delta_c = -1$, $\kappa = 10$, and $\eta = 15$.

of the induced optical lattice also increases; as a result, the width of the self-trapped wave packet deceases. This agrees with our variational discussion in the previous paragraph.

We also examined the stability of these self-trapped waves by directly simulating Eqs. (5) and (6). The results are shown in the right panels of Fig. 3. We found that for a weak pumping strength ($\eta = 6$ in the top panel), the induced optical lattice potential is not strong enough to retain the atoms around a single lattice site, they can tunnel to the neighboring sites, and the self-trapped wave packet spreads. When the pumping strength is strong ($\eta = 10, 15$ in the middle and bottom panels), the self-trapped wave packet can maintain its shape for quite a long time.

## IV. DYNAMICS

Because of the dissipative nature of the system, the moving dynamics of the self-trapped waves also show additional features. In the top panel of Fig. 4, we initially give the self-trapped wave packet a velocity of $v_0 = -3$ by imprinting a phase factor $\exp(-iv_0 x)$ on the steady state wave packet [51], and plot its density profile in the afterward evolution. Unlike the constant-speed moving of the conventional atomic bright soliton supported by interatom interaction ($s$-wave collision) [5], here we see that the self-trapped wave undergoes a decelerating motion. This is because according to Eqs. (5) and (6), there is a scope of timing delay between the change of light field and the moving of atomic condensate, and the condensate will feel a dragging (friction) force from the falling behind optical potential [46]. As shown in the bottom left panel, at $t = 0.5$ the center of the wave packet has traveled to $x = -1.23$ (black dashed line), but the bottom of the optical lattice is still left behind at $x = -0.89$, and the lattice will
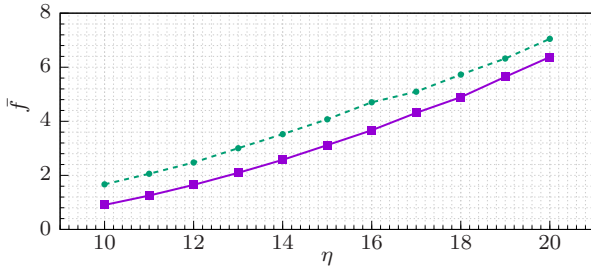
FIG. 5. Relation between mean friction force $\bar{f}$ and cavity pumping strength $\eta$. The squares and circles are data points collected from mean-field and semiclassical numerical simulations, respectively. The lines are simple linear connections of the data points to guide the eyes. Parameters used to plot this line are $U = -0.5$, $\Delta_c = -1$, $\kappa = 10$, and $v_0 = -3$.



FIG. 6. Relation between the mean friction force $\bar{f}$ and the initial wave packet moving speed $v_0$. The squares and circles are data points collected from mean-field and semiclassical numerical simulations, respectively. The lines are simple linear connections of the data points to guide the eyes. Parameters used to plot this line are $U = -0.5$, $\Delta_c = -1$, $\kappa = 10$, and $\eta = 15$.

impede the moving of the condensate. After traveling some distance, the self-trapped wave packet gets to stop, and the light field also catches up, thus the system comes back to a steady state (see bottom right panel of the figure where the center of the wave packet and the bottom of the lattice overlap again at $t = 5.0$).

This friction force can be used to cool atomic gas [19,20]. Moreover, it may also provide an opportunity to simplify the engineering of the self-trapped waves. For a conventional BEC bright soliton, if it is required to transfer from one place to another, one needs to firstly accelerate it, and then one also needs to slow down and stop it at the destination [52,53]. But for the self-trapped waves considered here, the stopping process can be omitted; one only needs to kick the self-trapped wave packet with an appropriate initial velocity, then it will travel to and stop at the destination automatically.

Next, we denote the mean friction force felt by the self-trapped wave as $\bar{f}$, and study its properties in detail. Its value can be calculated from equation

$$\bar{f} x_s = \frac{N m v_0^2}{2},  \tag{16}$$

where we equal the work done by the friction force and the initial kinetic energy of the self-trapped wave. And here $x_s$ is the limit traveling distance of the wave packet (as shown in Fig. 4), which is determined from numerical results.

We firstly examine the dependence of $\bar{f}$ on pumping strength $\eta$ (see Fig. 5). As the cavity pumping strength $\eta$ increases, the strength of the induced optical potential also increases accordingly. As can be expected, the self-trapped wave packet feels a stronger friction force at a larger pumping strength.

In Fig. 6, we plot $\bar{f}$ as a function of the initial speed $v_0$ of the self-trapped wave packet. The faster the self-trapped wave packet moves, the severer the light field falls behind, thus the friction force $\bar{f}$ is expected to be proportional to $v_0$. This is numerically observed at small values of $v_0$ ($v_0 < 3$). However, as $v_0$ further increases, the friction force is saturated; and after $v_0 > 6$ the friction force decreases. We found that this is caused by the escaping of atoms from the self-trapped wave packet. When the wave packet moves with a fast speed, a considerable fraction of atoms can escape from the self-trapped wave packet, thus the atomic density, and therefore the depth
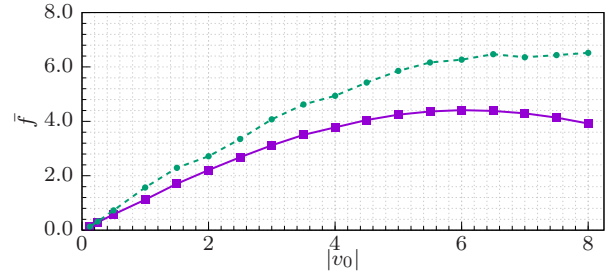
of the optical lattice is reduced. And a shallower optical lattice will have a weaker friction effect. This is shown in Fig. 7, in the left panel of which the evolution of atomic density for $v_0 = 8$ is plotted, and in the right panel the initial and final density profile is compared. In the figure, the escaping of atoms from the self-trapped wave packet is characterized by the precursor in the white box. And integrating the initial and final density profiles, we found that about 27% of the atoms have been lost.

Since the friction force results from the time delay of the cavity light field relative to the moving of the atomic matter wave, one can expect reducing the friction force by shortening the cavity relaxation time, i.e., increasing the cavity decay rate $\kappa$. This is also demonstrated by our numerical results (see Fig. 8), where the mean friction force $\bar{f}$ felt by the self-trapped wave is plotted as a function of the cavity decay rate $\kappa$.

And we also found that for a small value of the cavity decay rate $\kappa$, the moving dynamics of the self-trapped waves can show additional features. It undergoes a damped oscillation, as shown in Fig. 9. In the left panel, the moving of the density profile (colormap) and center position (black solid line) of the self-trapped wave is plotted. At the beginning stage, the delayed light field seriously decelerates the self-trapped wave packet. Because the light field falls too much behind in this
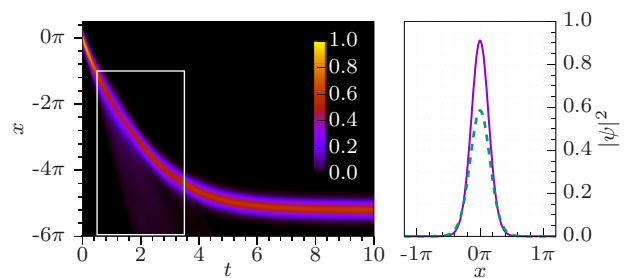


FIG. 7. Escaping of atoms from a fast-moving self-trapped wave packet. The initial speed of the wave packet is $v_0 = -8$. Left panel: Time evolution of the atomic density $|\psi|^2$. The escaping of atoms from the self-trapped wave packet is emphasized by the white box. Right panel: The initial ($t = 0$, violet solid line) and final ($t = 10$, green dashed line) density profiles of the self-trapped wave packet. Other parameters are $U = -0.5$, $\Delta_c = -1$, $\kappa = 10$, and $\eta = 15$.
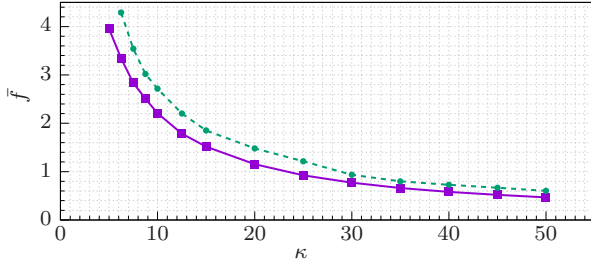
FIG. 8. Relation between the mean friction force $\bar{f}$ and decay rate of the cavity $\kappa$. The squares and circles are data points collected from mean-field and semiclassical numerical simulations, respectively. The lines are simple linear connections of the data points to guide the eyes. Parameters used to plot this line are $v_0 = -2$, $U = -0.5$, $\Delta_c = -1$, and $\eta = 15$.



FIG. 10. Constant-speed moving of the self-trapped wave packet in the bad cavity limit. To produce this figure, Eq. (6) together with bad cavity limit optical field formulas (8) and (9) are solved numerically. Parameters used are $v_0 = -2$, $U = -0.5$, $\Delta_c = -1$, $\eta = 75$, and $\kappa = 50$.

case, even the speed of the self-trapped wave packet has been decelerated to zero at $t = 0.96$ (the first minimal of the black solid line), the induced optical lattice potential still cannot catch up (see the right panel where we plot the density profile and the induced optical lattice potential at this time). As a result, in an afterward time interval the still falling behind optical lattice accelerates the self-trapped wave in the opposite direction. Then, the light field catches up, and decelerates the condensate again. This deceleration-acceleration process repeats several times, therefore the self-trapped wave undergoes a damped oscillation.

At last, in the bad cavity limit, the light field can instantaneously follow the moving self-trapped wave packet, thus it will have no friction effect on the self-trapped wave. In such a case, we expect that the self-trapped wave packet will move with its initial speed all the afterward time. In Fig. 10, the moving of a self-trapped wave packet is studied under the bad cavity approximation, i.e., the simulation is done by numerically solving Eqs. (6), (8), and (9). The expected constant speed motion is demonstrated by the numerical result.

## V. COMPARISON TO THE SEMICLASSICAL THEORY

Taking the atoms as classical polarizable particles, their motion can be approximately described by a one-dimensional Vlasov equation [20,21]

$$\frac{\partial f}{\partial t} + v \frac{\partial f}{\partial x} - \frac{\partial \mathcal{V}_{\text{eff}}}{\partial x} \frac{\partial f}{\partial v} = 0, \quad (17)$$

where $f(x, v, t)$ is the phase space distribution of the atoms where $v$ means the velocity. And the light field is still governed by Eq. (5), except that the variables $N_{\pm 1}$ and $N_{\pm 2}$ are now defined as

$$N_{\pm 1} = \int \rho(x) e^{\mp ix} dx$$

and

$$N_{\pm 2} = \int \rho(x) e^{\mp 2ix} dx,$$

with $\rho(x)$ being the spatial distribution of the atoms

$$\rho(x, t) = \int f(x, v, t) dv.$$

Such a semiclassical theory also predicts a self-trapped state of the atoms (see the left panel of Fig. 11). In this figure,
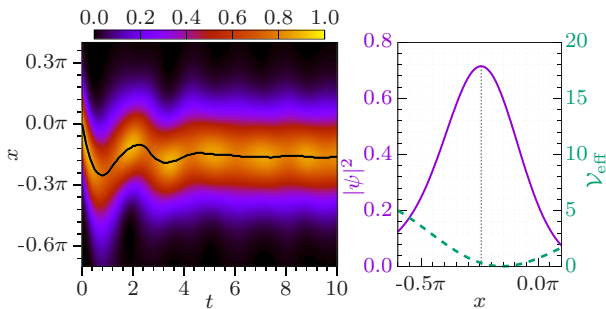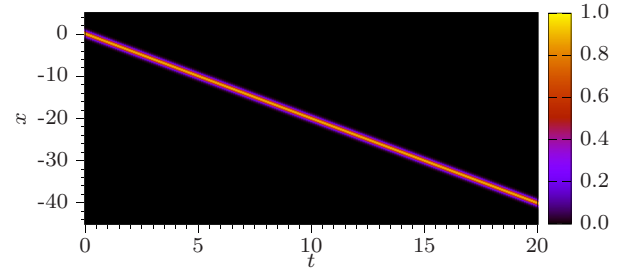


FIG. 9. Damped oscillation of the self-trapped wave packet under a small cavity decay rate ($\kappa = 2$). Left panel: Time evolution of the atomic density profile $|\psi|^2$. The black solid line is the center of the self-trapped wave packet. Right panel: Atomic density profile (violet solid line) and corresponding optical lattice potential (green dashed line) at $t = 0.96$ (the first time at which the speed of the wave packet reaches 0, i.e., the first minimal point of the black line in the left panel). The black dotted line is plotted to mark the center of the wave packet. Other parameters used are $v_0 = -2$, $U = -0.5$, $\Delta_c = -1$, and $\eta = 3$.
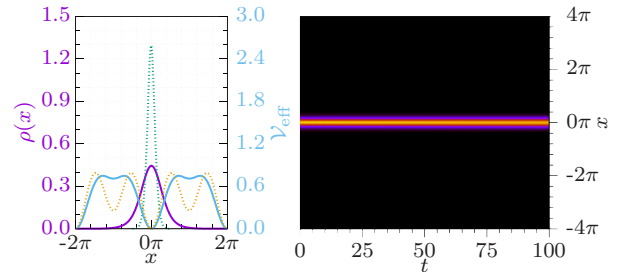


FIG. 11. A self-trapped state and its time evolution given by the semiclassical theory. Left panel: Spatial distribution (violet and green line) of the self-trapped state atoms and the corresponding optical lattice potential (cyan and brown line). The solid lines are the mean-field result, while the dotted lines are the semiclassical result. Right panel: Semiclassical time evolution of the self-trapped state. The parameters are $U = -0.5$, $\Delta_c = -1$, $\kappa = 10$, and $\eta = 6$, which are the same as in the top panels of Fig. 3.

we also plot the mean-field result for comparison. It is found that the semiclassical theory gives a narrower spatial distribution of the atoms than the mean-field theory. This is because the quantum pressure (the kinetic term in the Schödinger equation) which tends to spread the atomic distribution is absent in the semiclassical theory [while in the mean-field theory, the atoms are described by the Schrödinger-like equation (6) which can include the effect of quantum pressure].

Another difference between the mean-field and semiclassical theory results is the instability of the self-trapped state under weak pumping strength. Recall that under weak pumping strength tunneling of atoms to the neighboring lattice sites will lead to the spreading of the self-trapped state during its evolution (top right panel of Fig. 3). However, the semiclassical theory treats the atoms as classical particles, thus the tunneling phenomena cannot be included. As a result, it gives a nonspreading stable evolution of the self-trapped state (see the right panel of Fig. 11 where the parameters are chosen the same as in the top panels of Fig. 3).

We also compared the mean friction force predicted by mean-field and semiclassical theory, as shown in Figs. 5, 6, and 8. Because the semiclassical theory predicts a narrower spatial distribution of the atoms, the produced optical potential will also be tighter accordingly. And this will make the semiclassical theory overestimate the friction force.

## VI. SUMMARY

In summary, we have studied the self-trapped matter waves and their moving dynamics in a driven-dissipative ring cavity-BEC system within the mean-field theory. The self-trapped wave packets have been found by both variational and numerical methods, and the results fit with each other very well. The stability of the self-trapped waves is verified by direct numerical simulations. It is found that for a strong cavity pumping the self-trapped wave packet can be stable for quite a long time, while for a weak cavity pumping the self-trapped wave packet suffers a spatial spreading during its evolution. We also found that the moving dynamics of these self-trapped waves can be greatly affected by the cavity loss rate. Three distinct types of motion of the self-trapped waves have been identified in the system. For a cavity with a small decay rate, the cavity light field can alternatively drag and push the self-trapped wave packet, therefore the self-trapped wave packet endures a damped oscillation. And for a cavity with a moderate decay rate, the self-trapped wave packet always fells a dragging force from the cavity light field, and undergoes a decelerating motion. In the bad cavity limit, the friction force disappears, and the self-trapped wave packet constantly moves with the initial speed. The main results are also compared with a semiclassical calculation where the atoms are treated as classical particles. We found that the semiclassical theory predicts a narrower spatial distribution of the atoms, and will overestimate the friction force. It also misses the instability of the self-trapped state under weak pumping. These dynamical tunable self-trapped waves may find potential applications in fields such as matter wave interferometers [54–57].

[1] P. G. Drazin and R. S. Johnson, *Solitons: An Introduction*, 2nd ed. (Cambridge University Press, Cambridge, UK, 1989).

[2] B. Guo, X. F. Pang, Y. F. Wang, and N. Liu, *Solitons* (De Gruyter, Berlin/Boston, 2018).

[3] Y. S. Kivshar and G. P. Agrawal, *Optical Solitons* (Academic, San Diego, 2003).

[4] M. Kono and M. Skoric, *Nonlinear Physics of Plasmas* (Springer, Berlin/Heidelberg, 2010).

[5] P. G. Kevrekidis, D. J. Frantzeskakis, and R. Carretero-González, *Emergent Nonlinear Phenomena in Bose-Einstein Condensates: Theory and Experiment* (Springer, Berlin/Heidelberg, 2008).

[6] R. Carretero-González, D. J. Frantzeskakis, and P. G. Kevrekidis, Nonlinear waves in Bose-Einstein condensates: Physical relevance and mathematical techniques, Nonlinearity **21**, R139 (2008).

[7] M. Barranco, R. Guardiola, S. Hernández, R. Mayol, J. Navarro, and M. Pi, Helium nanodroplets: An overview, J. Low Temp. Phys. **142**, 1 (2006).

[8] F. Dalfovo, S. Giorgini, L. P. Pitaevskii, and S. Stringari, Theory of Bose-Einstein condensation in trapped gases, Rev. Mod. Phys. **71**, 463 (1999).

[9] L. Khaykovich, F. Schreck, G. Ferrari, T. Bourdel, J. Cubizolles, L. D. Carr, Y. Castin, and C. Salomon, Formation of a matter-wave bright soliton, Science **296**, 1290 (2002).

[10] K. E. Strecker, G. B. Partridge, A. G. Truscott, and R. G. Hulet, Formation and propagation of matter-wave soliton trains, Nature **417**, 150 (2002).

[11] K. E. Strecker, G. B. Partridge, A. G. Truscott, and R. G. Hulet, Bright matter wave solitons in Bose-Einstein condensates, New J. Phys. **5**, 73 (2003).

[12] T. D. Lee, K. Huang, and C. N. Yang, Eigenvalues and Eigenfunctions of a Bose System of Hard Spheres and its Low-Temperature Properties, Phys. Rev. **106**, 1135 (1957).

[13] H. Kadau, M. Schmitt, M. Wenzel, C. Wink, T. Maier, I. Ferrier-Barbut, and T. Pfau, Observing the Rosensweig instability of a quantum ferrofluid, Nature (London) **530**, 194 (2016).

[14] I. Ferrier-Barbut, H. Kadau, M. Schmitt, M. Wenzel, and T. Pfau, Observation of Quantum Droplets in a Strongly Dipolar Bose Gas, Phys. Rev. Lett. **116**, 215301 (2016).

[15] L. Chomaz, S. Baier, D. Petter, M. J. Mark, F. Wächtler, L. Santos, and F. Ferlaino, Quantum-Fluctuation-Driven Crossover from a Dilute Bose-Einstein Condensate to a Macro-droplet in a Dipolar Quantum Fluid, Phys. Rev. X **6**, 041039 (2016).

[16] C. R. Cabrera, L. Tanzi, J. Sanz, B. Naylor, P. Thomas, P. Cheiney, and L. Tarruell, Quantum liquid droplets in a mixture of Bose-Einstein condensates, Science **359**, 301 (2018).

[17] P. Cheiney, C. R. Cabrera, J. Sanz, B. Naylor, L. Tanzi, and L. Tarruell, Bright Soliton to Quantum Droplet Transition in a Mixture of Bose-Einstein Condensates, Phys. Rev. Lett. **120**, 135301 (2018).

[18] H. Ritsch, P. Domokos, F. Brennecke, and T. Esslinger, Cold atoms in cavity-generated dynamical optical potentials, Rev. Mod. Phys. **85**, 553 (2013).

[19] P. Domokos, P. Horak, and H. Ritsch, Semiclassical theory of cavity-assisted atom cooling, J. Phys. B: At., Mol. Opt. Phys. **34**, 187 (2001).

[20] W. Niedenzu, T. Grießer, and H. Ritsch, Kinetic theory of cavity cooling and self-organisation of a cold gas, Europhys. Lett. **96**, 43001 (2011).

[21] S. Ostermann, T. Grießer, and H. Ritsch, Atomic self-ordering in a ring cavity with counterpropagating pump fields, Europhys. Lett. **109**, 43001 (2015).

[22] J. Zhu, G. Dong, M. N. Shneider, and W. Zhang, Strong Local-Field Effect on the Dynamics of a Dilute Atomic Gas Irradiated by Two Counterpropagating Optical Fields: Beyond Standard Optical Lattices, Phys. Rev. Lett. **106**, 210403 (2011).

[23] K. Li, L. Deng, E. W. Hagley, M. G. Payne, and M. S. Zhan, Matter-Wave Self-Imaging by Atomic Center-of-Mass Motion Induced Interference, Phys. Rev. Lett. **101**, 250401 (2008).

[24] G. Dong, J. Zhu, W. Zhang, and B. A. Malomed, Polaritonic Solitons in a Bose-Einstein Condensate Trapped in a Soft Optical Lattice, Phys. Rev. Lett. **110**, 250401 (2013).

[25] M. A. Norcia, R. J. Lewis-Swan, J. R. K. Cline, B. Zhu, A. M. Rey, and J. K. Thompson, Cavity-mediated collective spin-exchange interactions in a strontium superradiant laser, Science **361**, 259 (2018).

[26] E. J. Davis, G. Bentsen, L. Homeier, T. Li, and M. H. Schleier-Smith, Photon-Mediated Spin-Exchange Dynamics of Spin-1 Atoms, Phys. Rev. Lett. **122**, 010405 (2019).

[27] Y. C. Zhang, V. Walther, and T. Pohl, Long-Range Interactions and Symmetry Breaking in Quantum Gases through Optical Feedback, Phys. Rev. Lett. **121**, 073604 (2018).

[28] X. Guan, J. Fan, X. Zhou, G. Chen, and S. Jia, Two-component lattice bosons with cavity-mediated long-range interaction, Phys. Rev. A **100**, 013617 (2019).

[29] G. R. M. Robb, E. Tesio, G. L. Oppo, W. J. Firth, T. Ackemann, and R. Bonifacio, Quantum Threshold for Optomechanical Self-Structuring in a Bose-Einstein Condensate, Phys. Rev. Lett. **114**, 173903 (2015).

[30] S. Ostermann, F. Piazza, and H. Ritsch, Spontaneous Crystallization of Light and Ultracold Atoms, Phys. Rev. X **6**, 021026 (2016).

[31] J. T. Mendonça and R. Kaiser, Photon Bubbles in Ultracold Matter, Phys. Rev. Lett. **108**, 033001 (2012).

[32] J. D. Rodrigues, J. A. Rodrigues, A. V. Ferreira, H. Terças, R. Kaiser, and J. T. Mendonça, Photon bubble turbulence in cold atomic gases, arXiv:1604.08114.

[33] L. Zhou, H. Pu, H. Y. Ling, and W. Zhang, Cavity-Mediated Strong Matter Wave Bistability in a Spin-1 Condensate, Phys. Rev. Lett. **103**, 160403 (2009).

[34] L. Zhou, H. Pu, H. Y. Ling, K. Zhang, and W. Zhang, Spin dynamics and domain formation of a spinor Bose-Einstein

condensate in an optical cavity, Phys. Rev. A **81**, 063641 (2010).

[35] L. Zhou, H. Pu, K. Zhang, X.-D. Zhao, and W. Zhang, Cavity-induced switching between localized and extended states in a noninteracting Bose-Einstein condensate, Phys. Rev. A **84**, 043606 (2011).

[36] A. Dalafi and M. H. Naderi, Intrinsic cross-Kerr nonlinearity in an optical cavity containing an interacting Bose-Einstein condensate, Phys. Rev. A **95**, 043601 (2017).

[37] M. Landini, N. Dogra, K. Kroeger, L. Hruby, T. Donner, and T. Esslinger, Formation of a Spin Texture in a Quantum Gas Coupled to a Cavity, Phys. Rev. Lett. **120**, 223602 (2018).

[38] S. Ostermann, H.-W. Lau, H. Ritsch, and F. Mivehvar, Cavity-induced emergent topological spin textures in a Bose-Einstein condensate, New J. Phys. **21**, 013029 (2019).

[39] M. Diver, G. R. M. Robb, and G.-L. Oppo, Nonlinear and chaotic dynamics of a Bose-Einstein condensate in an optical cavity, Phys. Rev. A **89**, 033602 (2014).

[40] Z.-C. Li, Q.-H. Jiang, Z. Lan, W. Zhang, and L. Zhou, Nonlinear Floquet dynamics of spinor condensates in an optical cavity: Cavity-amplified parametric resonance, Phys. Rev. A **100**, 033617 (2019).

[41] J. Qin, G. Dong, and B. A. Malomed, Hybrid Matter-Wave–Microwave Solitons Produced by the Local-Field Effect, Phys. Rev. Lett. **115**, 023901 (2015).

[42] J. Qin, Z. Liang, B. A. Malomed, and G. Dong, Tail-free self-accelerating solitons and vortices, Phys. Rev. A **99**, 023610 (2019).

[43] J. Qin, G. Dong, and B. A. Malomed, Stable giant vortex annuli in microwave-coupled atomic condensates, Phys. Rev. A **94**, 053611 (2016).

[44] F. Mivehvar, S. Ostermann, F. Piazza, and H. Ritsch, Driven-Dissipative Supersolid in a Ring Cavity, Phys. Rev. Lett. **120**, 123601 (2018).

[45] S. C. Schuster, P. Wolf, S. Ostermann, S. Slama, and C. Zimmermann, Supersolid Properties of a Bose-Einstein Condensate in a Ting Resonator, Phys. Rev. Lett. **124**, 143602 (2020).

[46] K. Gietka, F. Mivehvar, and H. Ritsch, Supersolid-Based Gravimeter in a Ring Cavity, Phys. Rev. Lett. **122**, 190801 (2019).

[47] P. Karpov and F. Piazza, Crystalline droplets with emergent color charge in many-body systems with sign-changing interactions, Phys. Rev. A **100**, 061401(R) (2019).

[48] J. I. Cirac, M. Lewenstein, and P. Zoller, Laser cooling a trapped atom in a cavity: Bad-cavity limit, Phys. Rev. A **51**, 1650 (1995).

[49] P. Horak, S. M. Barnett, and H. Ritsch, Coherent dynamics of Bose-Einstein condensates in high-finesse optical cavities, Phys. Rev. A **61**, 033609 (2000).

[50] J. M. Zhang, W. M. Liu, and D. L. Zhou, Mean-field dynamics of a Bose Josephson junction in an optical cavity, Phys. Rev. A **78**, 043618 (2008).

[51] J. Denschlag, J. E. Simsarian, D. L. Feder, C. W. Clark, L. A. Collins, J. Cubizolles, L. Deng, E. W. Hagley, K. Helmerson, W. P. Reinhardt, S. L. Rolston, B. I. Schneider, and W. D. Phillips, Generating solitons by phase engineering of a Bose-Einstein condensate, Science **287**, 97 (2000).

[52] P. G. Kevrekidis, D. J. Frantzeskakis, R. Carretero-González, B. A. Malomed, G. Herring, and A. R. Bishop, Statics, dynam-

ics, and manipulations of bright matter-wave solitons in optical lattices, Phys. Rev. A **71**, 023614 (2005).

[53] L. W. S. Baines and R. A. Van Gorder, Soliton wave-speed management: Slowing, stopping, or reversing a solitary wave, Phys. Rev. A **97**, 063814 (2018).

[54] J. Polo and V. Ahufinger, Soliton-based matter-wave interferometer, Phys. Rev. A **88**, 053628 (2013).

[55] G. D. McDonald, C. C. N. Kuhn, K. S. Hardman, S. Bennetts, P. J. Everitt, P. A. Altin, J. E. Debs, J. D. Close, and N. P. Robins, Bright Solitonic Matter-Wave Interferometer, Phys. Rev. Lett. **113**, 013002 (2014).

[56] J. L. Helm, S. L. Cornish, and S. A. Gardiner, Sagnac Interferometry Using Bright Matter-Wave Solitons, Phys. Rev. Lett. **114**, 134101 (2015).

[57] O. J. Wales, A. Rakonjac, T. P. Billam, J. L. Helm, S. A. Gardiner, and S. L. Cornish, Splitting and recombination of bright-solitary-matter waves, Commun. Phys. **3**, 51 (2020).